Analytical solution for nonlinear consolidation of combined electroosmosis-vacuum-surcharge preloading

Article *in* Computers and Geotechnics · May 2020

DOI: 10.1016/j.compgeo.2020.103484

CITATIONS
0

READS
80

4 authors, including:

Liujiang Wang
Hohai University
23 PUBLICATIONS **144** CITATIONS

SEE PROFILE

Sihong Liu
Hohai University
93 PUBLICATIONS **837** CITATIONS

SEE PROFILE

Eduardo Alonso
Universitat Politècnica de Catalunya
62 PUBLICATIONS **1,560** CITATIONS

SEE PROFILE

Computers and Geotechnics 121 (2020) 103484

Contents lists available at ScienceDirect

Computers and Geotechnics

journal homepage: www.elsevier.com/locate/compgeo

Research Paper

Analytical solution for nonlinear consolidation of combined electroosmosis-vacuum-surcharge preloading

Liujiang Wang[a,*], Penghua Huang[a], Sihong Liu[a], Eduardo Alonso[b]

[a] College of Water Conservancy and Hydropower, Hohai University, Nanjing 210098, China
[b] Department of Geotechnical Engineering and Geosciences, Universitat Politecnica de Catalunya, Barcelona, Spain

ARTICLE INFO

Keywords:
Vacuum-surcharge preloading
Electroosmosis
Nonlinearity
Vertical drains
Consolidation

ABSTRACT

In this study, analytical solutions of the consolidation of vertical drains combined with electroosmosis-vacuum-surcharge preloading are derived considering void ratio-dependent compressibility, hydraulic permeability and permeability of electroosmosis. In addition, radial and vertical flow, changes of the hydraulic and electroosmosis permeabilities in the smear zone, and time-dependent surcharge preloading are also considered. The solution is verified by comparing it with experimental result and numerical solution in the previous literature. Finally, a parametric study is conducted to investigate the influence of considering nonlinearity, smear zone, and non-synchronous change of hydraulic and electroosmosis permeability in void ratio. The result indicates that the average negative pore water pressure under combined electroosmosis-vacuum-surcharge preloading is larger with the consideration of nonlinear change of the soil parameters, and the consolidation rate is also faster. The presence of a smear zone decreases the consolidation rate and increases the final settlement. A slower consolidation rate is obtained for the smear zone with the large radius and the less permeable. The consolidation rate, final settlement and negative pore water pressure increase for the soils with the large value of electro-osmosis permeability index. In addition, the decrease of the vertical hydraulic permeability will increase the final settlement and consolidation time.

1. Introduction

Vacuum pressure and surcharge preloading combined with prefabricated vertical drains (PVDs) is widely used to improve mechanical properties of soft soil [1–4]. This method accelerates the consolidation process of soft soil by shortening the drainage path [5,6] and increasing hydraulic gradient, resulting in lower water content and higher effective stress [7,8]. Although this method is identified as a workable solution in the soil consolidation, and the reinforcement results are satisfactory for silty soils, but not for clayey soils or other fine deposits [9,10]. In the clayey soil conditions, a portion of the clay drifts under the applied vacuum pressure and forms clogs in the surrounding of the drains [11,12]. Though this clogging layer is thin, it severely restricts the vacuum pressure to a limited zone of influence and obstructs the efficient flow of water [13]. In addition, this process is time dependent for clayey soils, which leads to less viable for meeting goals when time is taking as controlling factor. Moreover, the timing issue escalates the process of deciding where to consolidate a clayey soil layer with large thickness. Nowadays, the depth of the deposit, which ranges from metres to tens of metres, usually occurs in cases of estuarine reclamation, sewage slurry and mine waste dumps. Therefore, to accelerate the consolidation rate, a novel method is proposed to combine the electroosmosis with the vacuum-surcharge preloading [14]. The electroosmosis has been shown an effective method in driving a stream of water through clayed soils with low permeability [15], and its performance can effectively complement the shortage of vacuum-surcharge preloading, as reported in various studies [11,14,16]. Furthermore, since the negative pore water pressure induced by the electroosmosis can counteract the excess pore water pressure caused by the surcharge loading, which will reduce the risk of shear failure of the treated soft foundation further.

The setup of the electroosmosis-vacuum-surcharge preloading process is illustrated in Fig. 1. Added to the vacuum-surcharge preloading system is an array of electrodes that are installed in the soil layer of interest. The cathodes use the electro-kinetic vertical drains (EVD), and the anodes are installed between the drains. Although the anodes and cathodes can line up [17], to facilitate their installations, the electrodes are often laid out in a triangular pattern, as illustrated in Fig. 1(b), enabling a radial flow mode and efficient drainage. For a cell of coupled radial-vertical flow, the zone of influence and its profile view, which

* Corresponding author at: College of Water Conservancy and Hydropower, Hohai University, Xikang Road 1, Nanjing 210098, China.
E-mail address: 15850514642@163.com (L. Wang).

https://doi.org/10.1016/j.compgeo.2020.103484
Received 19 November 2019; Received in revised form 16 January 2020; Accepted 9 February 2020

Notations

A	governing equation parameter
A_0	constant parameter
A_1	constant parameter
$\overline{A}$	simplified governing equation parameter
B	governing equation parameter
B_0	constant parameter
B_1	constant parameter
$\bar{B}$	simplified governing equation parameter
C	governing equation parameter
$\bar{C}$	simplified governing equation parameter
C_c	compressive index
C_{kh}	radial hydraulic permeability index
C_{kv}	vertical hydraulic permeability index
C_{ke}	electroosmosis permeability index
e	void ratio
e_0	initial void ratio
E_a	constant parameter of smear zone
F_a	constant parameter of smear zone
$f_1(r)$	distribution function of hydraulic permeability coefficient
$f_2(r)$	distribution function of electroosmosis permeability coefficient
$g(r)$	ratio of $f_1(r)$ to $f_2(r)$
H	soil depth
i	number of ith surcharge loading
k_h	radial hydraulic permeability coefficient
k_{h0}	initial radial hydraulic permeability coefficient
k_{hr}	radial hydraulic permeability coefficient in the smear zone
k_v	vertical hydraulic permeability coefficient
k_{v0}	initial vertical hydraulic permeability coefficient
k_e	electroosmosis permeability coefficient
k_{e0}	initial electroosmosis permeability coefficient
k_{er}	electroosmosis permeability coefficient in the smear zone
k_1	reduction factor of vacuum degree along depth
m	summation index
m_{v0}	initial volumetric compressibility coefficient
M	eigenvalue
n	the ratio of r_e to r_w
$p(z)$	vacuum pressure along the depth
p_v	applied vacuum pressure
$q(t)$	surcharge loading
q_0	initial surcharge loading
q_f	final surcharge loading
r	radii
r_e	radii of influence zone
r_s	radii of smear zone
r_w	radii of vertical drain
R_i	ith surcharge loading rate
s	the ratio of r_s to r_w
S	settlement
t	time
t_1	single stage surcharge loading time
u	excess pore water pressure
$\overline{u}$	average excess pore water pressure at any depth
$\overline{u}_{eo}^{ult}$	final pore water pressure induced by electroosmosis only
U_s	degree of consolidation
U_p	degree of dissipation
v_r	flow velocity in the radial direction
v_z	flow velocity in the vertical direction
$V(r)$	distribution function of potential
z	vertical coordinate
η_1	the ratio of k_h to k_{hr}
η_2	the ratio of k_e to k_{er}
$\overline{\sigma}'$	average effective stress
$\overline{\sigma}_0'$	initial average effective stress
τ	Variable of time integration
ξ	transform variable
γ_w	unit weight of water
ε_v	volumetric strain
β_m	eigen equation
ϕ_a	applied voltage
Δe	increment of void ratio

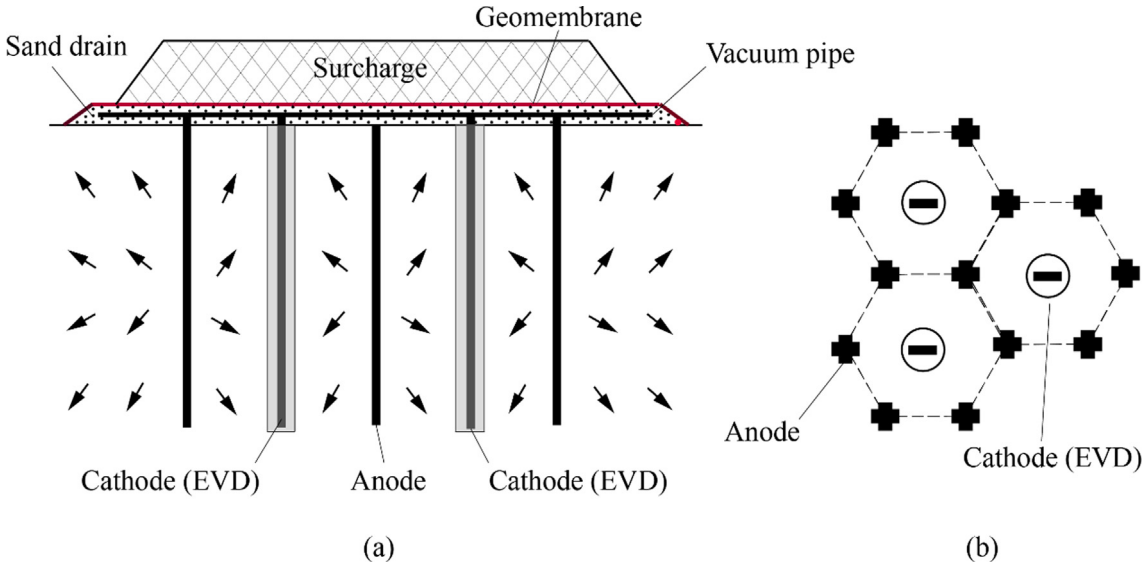

Fig. 1. Schematic of electroosmosis-vacuum-surcharge preloading installation: (a) profile, and (b) triangular layout of PVDs-electrodes.

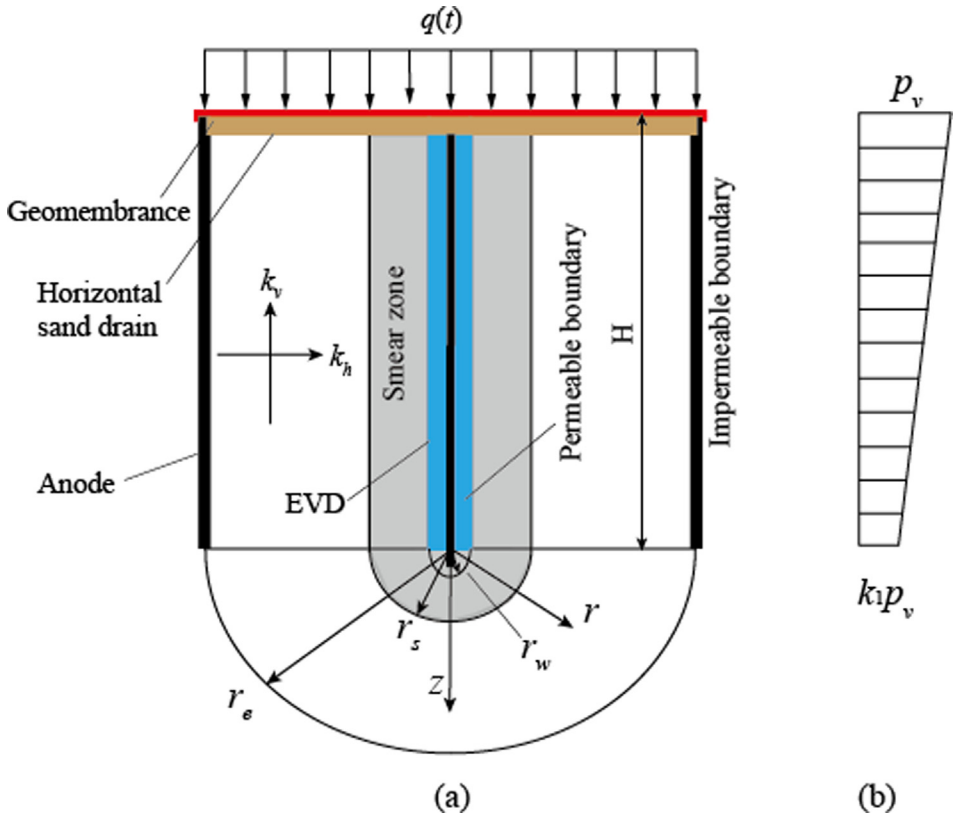

Fig. 2. (a) Analysis schemes of unit cells with an EVD under electroosmosis-vacuum-surcharge preloading; (b) Trapezoidal vacuum pressure along the drain boundary.

includes the soil layer conditions, is provided in Fig. 2.

The theory of soil consolidation improved by electroosmosis related methods in the cell was initially studied by Wan and Mitchell [18]. Their model only considered the electroosmosis-surcharge preloading process. Besides, to simplify the process, they sealed the top and bottom boundaries to enable only the horizontal flow of water. Therefore, two-dimensional (2D) models were developed to consider the horizontal and vertical flows simultaneously [19,20]. Furthermore, an axisymmetric analytical model for the electroosmosis was proposed ignoring the equal strain hypothesis with the consideration of the coupled radial-vertical seepage [21]. For the consolidation under combined action of electroosmosis-vacuum preloading, the 2D analytical models have been proposed, which could consider the coupled horizontal-vertical flow and time-dependent reduction of applied voltage were proposed [22,23]. Recently, an axisymmetric analytical model for combined electroosmosis-vacuum-surcharge preloading was developed [24], with the smear zone, reduction of vacuum pressure along the vertical drains, surcharge loading process and distribution of additional stress in the soil layers considered in their model. Although some progress has been made on the consolidation behavior of vertical drains of electroosmosis and related methods with the combination of vacuum and surcharge preloading, few analytical solutions for electroosmosis consolidation allow for the effect of soil nonlinearity. When the soil layer is thick and large deformation has occurred [25], the soil properties vary in the course of consolidation, which invalidates the constant-property assumption.

To consider the varying soil properties, the finite element method was used to simulate one-dimensional (1D) [26] and 2D consolidation problems [27]. In addition, the finite difference method was also used to develop a 1D electroosmosis consolidation model (EC1), a 2D model (EC2) and an axisymmetric model (EC3) [28–30]. However, these numerical methods are difficult for engineers to use in an actual design, and analytical solution is more acceptable. Thus, an analytical model for consolidation under electroosmosis-surcharge was proposed [31] within the framework of large strain consolidation theory [32]. After that, analytical models with the consideration of the nonlinear variation of soil compressibility, hydraulic and electroosmosis permeability in soil deformation and degree of saturation were developed [33,34], respectively. Their studies, however, were applied to the simplified 1D layout of anodes and cathode drains and are not applicable to the triangular layout pattern. Thus, analytical model for the nonlinear consolidation arising from the triangular layout pattern requires further examination.

In this paper, an analytical model for electroosmosis-vacuum-surcharge preloading was proposed to consider the effect of nonlinearity change of compressibility, hydraulic permeability and electroosmosis permeability with void ratio, based on the previous studies on the consolidation theory of vertical drains [35–37]. Radial and vertical flow, different changes of the hydraulic and electroosmosis permeabilities in the smear zone, and time-dependent surcharge preloading were considered. Then, the capability of the proposed analytical model was validated against experimental results and numerical solutions. Finally, a parametric study was conducted to investigate the influences of the compressibility index, applied voltage, and surcharge loading type with and without considering nonlinearity. Besides, the influences of the radius and soil permeability of the smear zone, non-synchronous variation of hydraulic and electroosmosis permeability in void ratio, and variation of vertical hydraulic permeability were studied.

2. Mathematical model, governing equations and analytical solution

2.1. Mathematic model

The axisymmetric unit cell model is presented in Fig. 2. The soil layer, which is H in thickness, is subjected to a surcharge load, q(t),

vacuum pressure, p(z), and an electric field with voltage, V(r). The coordinate z is the vertical distance from the soil surface and positive downward. The zone of influence is subdivided into three sections: the native soil, the smear zone, and the drain, all in the radial direction. The three sections, in the form of concentric cylinders, correspond to the radii r_e, r_s, and r_w. Meanwhile, k_h and k_v are the radial and vertical hydraulic permeability coefficient, respectively. To derive the analytical solution, the following assumptions are adopted:

(1) The soil is assumed to be fully saturated and Darcy's law is valid. At the outer boundary of the model, the water flow is not allowed. Both water and soil particles are incompressible.
(2) In according with the concept of equal-strain [38], vertical strains at the same depth within the unit cell are assumed to be the same and only the vertical strains are considered.
(3) The velocity of pore water flow due to electroosmosis is directly proportional to the electrical gradient, and can be linearly superimposed with that due to hydraulic gradient [39].
(4) The pore water flow caused by thermal gradient and chemical concentration gradient is neglected.
(5) The total stress induced by the surcharge load is uniformly distributed along the depth.

2.2. Governing equation

Combining the assumption in previous studies [36,40] that the vacuum pressure decreases linearly along the drain, the vacuum pressure at the drain boundary is assumed to vary with depth, which can be expressed as:

$$p = p_v\left[1 - (1 - k_1)\frac{z}{H}\right] \tag{1}$$

where p is the vacuum pressure along the vertical drain, k_1 is the constant to depict the decrease of vacuum pressure along depth, p_v is the design vacuum pressure.

To reflect the nonlinearity relationships of compressibility, hydraulic permeability and electroosmosis permeability in void ratio, the following functions are adopted as [28,29,33]:

$$e = e_0 - C_c\log\left(\frac{\overline{\sigma}'}{\overline{\sigma}'_0}\right) \tag{2a}$$

$$e = e_0 + C_{kh}\log\left(\frac{k_h}{k_{h0}}\right) \tag{2b}$$

$$e = e_0 + C_{kv}\log\left(\frac{k_v}{k_{v0}}\right) \tag{2c}$$

$$e = e_0 + C_{ke}\log\left(\frac{k_e}{k_{e0}}\right) \tag{2d}$$

where C_c is the compressive index; C_{kh}, C_{kv} and C_{ke} are the radial and vertical hydraulic permeability index, and electroosmosis permeability index; k_h and k_{h0} are the radial permeability coefficients of the undisturbed soils at any time and at initial time, respectively; k_v and k_{v0} are the vertical permeability coefficients of the undisturbed soil at any time and at initial time; k_e and k_{e0} are the electroosmosis permeability coefficients of the undisturbed soil at any time and at initial time; e and e_0 are the void ratio at any time and at the initial time, respectively; $\overline{\sigma}'$ and $\overline{\sigma}'_0$ are the average effective stress at any time and at initial time.

There are several different patterns for distributions of permeable coefficient in smear zone [41]. Noting that, the decrease of the hydraulic permeability in smear zone is larger than that of electroosmosis permeability [33]. For simplification, both radial hydraulic and electroosmosis permeability coefficients along the radial direction are step distributed, which can be expressed as:

$$k_{hr} = k_h f_1(r) \tag{3a}$$

$$k_{er} = k_e f_2(r) \tag{3b}$$

$$f_1(r) = \begin{cases}\frac{1}{\eta_1} r_w < r < r_s\\ 1 r_s < r < r_e\end{cases} \tag{3c}$$

$$f_2(r) = \begin{cases}\frac{1}{\eta_2} r_w < r < r_s\\ 1 r_s < r < r_e\end{cases} \tag{3d}$$

where $\eta_1 = \frac{k_h}{k_{hr}|_{r=r_w}}$, $\eta_2 = \frac{k_e}{k_{er}|_{r=r_w}}$.

Following the previous literatures [39], the combined pore water flow velocity in the radial and vertical directions under the hydraulic gradient and electrical gradient can be described as:

$$\begin{cases} v_r = \frac{k_h f_1(r)}{\gamma_w}\frac{\partial u}{\partial r} + k_e f_2(r)\frac{\partial V}{\partial r}\\ v_z = \frac{k_v}{\gamma_w}\frac{\partial u}{\partial z}\end{cases} \tag{4}$$

where u is the excess pore water pressure; V is the electrical potential along the radial direction; γ_w is the unit weight of water; v_r and v_z are the pore water flow velocity in the radial and vertical directions.

According to Eq. (4), we defined a new variable as [24]:

$$\xi = u + \frac{\gamma_w k_e}{k_h} V(r) g(r) \tag{5a}$$

$$V(r) = \frac{\ln(r/r_w)}{\ln(r_e/r_w)}\phi_a \tag{5b}$$

$$g(r) = \frac{f_2(r)}{f_1(r)} = \begin{cases}\frac{\eta_1}{\eta_2} r_w < r < r_s\\ 1 r_s < r < r_e\end{cases} \tag{5c}$$

where ϕ_a is the design voltage applied in the system.

Following the previous work [42], the governing equation for the nonlinear consolidation of soil improved by combined electroosmosis-vacuum-surcharge preloading can be expressed as follows:

$$\frac{1}{r}\frac{\partial}{\partial r}\left\{\frac{k_h f_1(r)}{\gamma_w} r\frac{\partial \xi}{\partial r}\right\} + \frac{k_v}{\gamma_w}\frac{\partial^2 \overline{u}}{\partial z^2} = -\frac{\partial \varepsilon_v}{\partial t} \tag{6}$$

where $\overline{u}$ is the average excess pore water pressure in the soil at any depth, ε_v is the vertical strain of the soil.

The boundary and initial conditions are as follows:

$$\begin{cases} r = r_e \frac{\partial \xi}{\partial r} = 0\\ r = r_w \xi = p(z)\\ z = 0 \overline{u} = p_v\\ z = H \frac{\partial \overline{u}}{\partial z} = 0\\ t = 0 \overline{u} = q(0) = q_0\end{cases} \tag{7}$$

Integrating Eq. (6) from r to r_e and combining it with boundary condition in the radial direction at $r = r_e$ yields:

$$\frac{\partial \xi}{\partial r} = \frac{\gamma_w}{2k_h}\left(\frac{\partial \varepsilon_v}{\partial t} + \frac{k_v}{\gamma_w}\frac{\partial^2 \overline{u}}{\partial z^2}\right)\left(\frac{r_e^2}{r f_1(r)} - \frac{r}{f_1(r)}\right) \tag{8}$$

By integrating Eq. (8) again from r_w to r and combining it with the boundary condition $r = r_w$, the variable ξ can be derived as follows:

$$\xi = p(z) + \frac{\gamma_w}{2k_h}\left(\frac{\partial \varepsilon_v}{\partial t} + \frac{k_v}{\gamma_w}\frac{\partial^2 \overline{u}}{\partial z^2}\right)(A_0 r_e^2 - B_0) \tag{9}$$

where $A_0 = \int_{r_w}^{r} \frac{1}{r f_1(r)} dr$, $B_0 = \int_{r_w}^{r} \frac{r}{f_1(r)} dr$.

Based on the equal strain assumption, the average excess pore water pressure in the soil at any depth can be expressed as follows:

$$\overline{u} = \frac{1}{\pi(r_e^2 - r_w^2)} \int_{r_w}^{r_e} 2\pi r u dr \tag{10}$$

Combining Eq. (5a) and Eq. (9), the excess pore water pressure u can be obtained and substituted into Eq. (10) yields:

$$\overline{u} = p(z) + \frac{\gamma_w r_e^2 F_a}{2k_h}\left(\frac{\partial \varepsilon_v}{\partial t} + \frac{k_v}{\gamma_w}\frac{\partial^2 \overline{u}}{\partial z^2}\right) - C \tag{11}$$

where

$$F_a = \frac{2(A_1 r_e^2 - B_1)}{r_e^2(r_e^2 - r_w^2)} \tag{12a}$$

$$A_1 = \int_{r_w}^{r_e} r A_0(r) dr \tag{12b}$$

$$B_1 = \int_{r_w}^{r_e} r B_0(r) dr \tag{12c}$$

$$C = \frac{2k_e \gamma_w}{k_h} E_a \tag{12d}$$

$$E_a = \frac{1}{(r_e^2 - r_w^2)} \int_{r_w}^{r_e} r V(r) g(r) dr \tag{12e}$$

Substituting Eq. (3c) into A_1, B_1, and F_a, the value of F_a can be expressed as:

$$F_a = \frac{n^2}{n^2 - 1}\left[\ln(n) - \frac{3}{4} + \frac{1}{n^2} - \frac{1}{4n^4} + (\eta_1 - 1)\left(\ln(s) + \frac{1 - s^2}{n^2} + \frac{s^4 - 1}{4n^4}\right)\right] \tag{13}$$

where $n = r_e/r_w$, $s = r_s/r_w$.

Substituting Eqs. (5b), (5c) into E_a, the value of E_a can be expressed as:

$$E_a = \frac{\phi_a}{(n^2 - 1)\ln(n)}\left[\left(\frac{\eta_1}{\eta_2} - 1\right)\left(\frac{s^2 \ln(s)}{2} + \frac{1 - s^2}{4}\right) + \left(\frac{n^2 \ln(n)}{2} + \frac{1 - n^2}{4}\right)\right] \tag{14}$$

Combining the nonlinear compressive relationship, the rate of deformation can be expressed as:

$$\frac{\partial \varepsilon_v}{\partial t} = -\frac{1}{1 + e_0}\frac{\partial e}{\partial t} = \frac{C_c}{(1 + e_0)\ln(10)}\frac{1}{\overline{\sigma}'}\frac{\partial \overline{\sigma}'}{\partial t} = m_{v0}\frac{\overline{\sigma}'_0}{\overline{\sigma}'}\frac{\partial \overline{\sigma}'}{\partial t} \tag{15}$$

where m_{v0} is the initial volumetric compressibility coefficient.

Taking Eqs. (2b), (2c), (2d), (12d) and (15) into Eq. (11), the average excess pore water pressure can be obtained as:

$$\overline{u} = p(z) + \frac{\gamma_w r_e^2 F_a m_{v0}}{2k_{h0}}\left(\frac{\overline{\sigma}'}{\overline{\sigma}'_0}\right)^{\frac{C_c}{C_{kh}} - 1}\frac{\partial \overline{\sigma}'}{\partial t} + \frac{k_{v0} r_e^2 F_a}{2k_{h0}}\left(\frac{\overline{\sigma}'}{\overline{\sigma}'_0}\right)^{\frac{C_c}{C_{kh}} - \frac{C_c}{C_{kv}}}\frac{\partial^2 \overline{u}}{\partial z^2} - \frac{2k_{e0}\gamma_w E_a}{k_{h0}}\left(\frac{\overline{\sigma}'}{\overline{\sigma}'_0}\right)^{\frac{C_c}{C_{kh}} - \frac{C_c}{C_{ke}}} \tag{16}$$

Based on the principle of effective stress, the average effective stress can be obtained as:

$$\overline{\sigma}' = \overline{\sigma}'_0 + q(t) - \overline{u} \tag{17}$$

Substituting Eq. (17) into Eq. (16) leads to:

$$A\frac{\partial^2 \overline{u}}{\partial z^2} - B\frac{\partial \overline{u}}{\partial t} - \overline{u} = -p(z) + C - B\frac{\partial q}{\partial t} \tag{18}$$

where

$$A = \frac{k_{v0} r_e^2 F_a}{2k_{h0}}\left(\frac{\overline{\sigma}'}{\overline{\sigma}'_0}\right)^{\frac{C_c}{C_{kh}} - \frac{C_c}{C_{kv}}} \tag{19a}$$

$$B = \frac{\gamma_w r_e^2 F_a m_{v0}}{2k_{h0}}\left(\frac{\overline{\sigma}'}{\overline{\sigma}'_0}\right)^{\frac{C_c}{C_{kh}} - 1} \tag{19b}$$

$$C = \frac{2k_{e0}\gamma_w E_a}{k_{h0}}\left(\frac{\overline{\sigma}'}{\overline{\sigma}'_0}\right)^{\frac{C_c}{C_{kh}} - \frac{C_c}{C_{ke}}} \tag{19c}$$

Obviously, solving Eq. (18) analytically is difficult with varying coefficients. Therefore, the simplified approach [35,36] was adopted by replacing $\overline{\sigma}'/\overline{\sigma}'_0$ with the approximation $[\overline{\sigma}'_0 + \overline{\sigma}'_{t=+\infty}]/2\overline{\sigma}'_0$. Thus, $\overline{\sigma}'$ is removed and the variable coefficients of the nonlinear partial differential equations are changed into constant coefficients, allowing Eq. (18) to be solved analytically. This simplifies the problem substantially and can provide an explicit analytical solution. Despite the simplification, the predicted results from the analytical solution were consistent with data measured in the laboratory tests [36].

For consolidation under combined electroosmosis-vacuum-surcharge preloading, the final effective stress can be expressed as:

$$\overline{\sigma}'_{t=+\infty} = \overline{\sigma}'_0 + q_f - \frac{p_v}{2}(1 + k_1) - \overline{u}_{eo}^{ult} \tag{20}$$

where q_f is the final surcharge loading; $\overline{u}_{eo}^{ult}$ is the final pore water pressure induced by electroosmosis merely, the details of derivation of $\overline{u}_{eo}^{ult}$ is shown in Appendix A.

By replacing $\overline{\sigma}'/\overline{\sigma}'_0$ with its average value, the Eq. (18) is reduced to:

$$\overline{A}\frac{\partial^2 \overline{u}}{\partial z^2} - \overline{B}\frac{\partial \overline{u}}{\partial t} - \overline{u} = -p(z) + \overline{C} - \overline{B}\frac{\partial q}{\partial t} \tag{21}$$

where

$$\overline{A} = \frac{k_{v0} r_e^2 F_a}{2k_{h0}}\left\{\frac{\overline{\sigma}'_0 + \left[\overline{\sigma}'_0 + q_f - \frac{p_v}{2}(1 + k_1) - \overline{u}_{eo}^{ult}\right]}{2\overline{\sigma}'_0}\right\}^{\frac{C_c}{C_{kh}} - \frac{C_c}{C_{kv}}} \tag{22a}$$

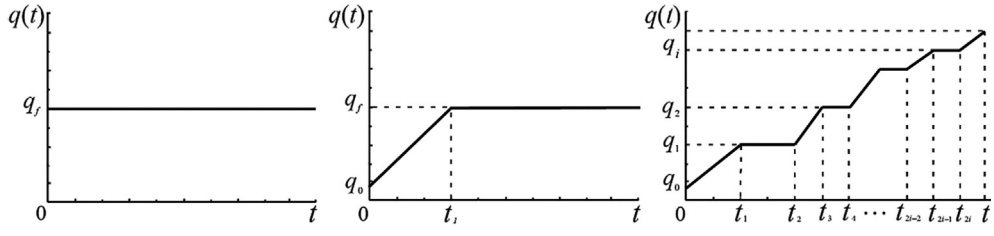

(a) Instantaneous loading (b) Single-stage loading (c) Multi-stage loading

Fig. 3. Surcharge loading types.

$$\overline{B} = \frac{\gamma_w r_e^2 F_a m_{v0}}{2k_{h0}} \left\{ \frac{\overline{\sigma}'_0 + \left[\overline{\sigma}'_0 + q_f - \frac{p_v}{2}(1+k_1) - \overline{u}_{eo}^{ult}\right]}{2\overline{\sigma}'_0} \right\}^{\frac{C_c}{C_{kh}}-1} \tag{22b}$$

$$\overline{C} = \frac{2k_{e0}\gamma_w E_a}{k_{h0}} \left\{ \frac{\overline{\sigma}'_0 + \left[\overline{\sigma}'_0 + q_f - \frac{p_v}{2}(1+k_1) - \overline{u}_{eo}^{ult}\right]}{2\overline{\sigma}'_0} \right\}^{\frac{C_c}{C_{kh}}-\frac{C_c}{C_{ke}}} \tag{22c}$$

2.3. Analytical solutions of excess pore water pressure for several special cases

Based on the method of separation of variables and combining with the boundary conditions and initial condition in Eq. (7), the solution for average pore water pressure can be obtained as:

$$\overline{u}(z,t) = p_v + \sum_{m=1}^{\infty} e^{-\beta_m t}\left[\int_0^t Q_m(\tau)e^{\beta_m \tau}d\tau + \frac{2(q_0-p_v)}{M}\right]\sin\left(\frac{M}{H}z\right) \tag{23}$$

where

$$M = \frac{2m-1}{2}\pi, \quad m = 1, 2, 3. .. \tag{24a}$$

$$\beta_m = \frac{\overline{A}M^2}{\overline{B}H^2} + \frac{1}{\overline{B}} \tag{24b}$$

$$Q_m = -\frac{2}{M\overline{B}}\left[\overline{C} + \frac{(-1)^{m+1}p_v(1-k_1)}{M}\right] + \frac{2}{M}\frac{\partial q}{\partial t} \tag{24c}$$

where m is the summation index; and M is the eigenvalue.

2.3.1. Instantaneous loading

As shown in Fig. 3a, the surcharge preloading is applied instantaneously and kept constant through the whole process, which can be expressed as:

$$q(t) = q_0 = q_f \tag{25}$$

Substituting Eq. (25) into Eq. (24b), and then taking Eq. (24b) into Eq. (23) leads to:

$$\overline{u}(z,t) = p_v + \sum_{m=1}^{\infty}\frac{2}{M}\left[\begin{array}{c}(q_0-p_v)e^{-\beta_m t} \\ -\frac{1}{\beta_m\overline{B}}\left[\overline{C} + \frac{(-1)^{m+1}p_v(1-k_1)}{M}\right](1-e^{-\beta_m t})\end{array}\right]\sin\left(\frac{M}{H}z\right) \tag{26}$$

2.3.2. Single-stage loading

As shown in Fig. 3b, the surcharge preloading is gradually applied by a single-stage pattern. The surcharge pressure increases to the final value in a linear way when $t < t_1$ and keeps constant after t_1, which can be described as:

$$q(t) = \begin{cases} \frac{q_f - q_0}{t_1}t & t < t_1 \\ q_f \; t \geqslant t_1 \end{cases} \tag{27}$$

Substituting Eq. (27) into Eqs. (24b) and (23) leads to:

$$\overline{u}(z,t) = \begin{cases} p_v + \sum_{m=1}^{\infty}\frac{2}{M}\left[\begin{array}{c}(q_0-p_v)e^{-\beta_m t} + \frac{(q_f-q_0)(1-e^{-\beta_m t})}{\beta_m t_1} \\ -\frac{1}{\beta_m\overline{B}}\left[\overline{C} + \frac{(-1)^{m+1}p_v(1-k_1)}{M}\right](1-e^{-\beta_m t})\end{array}\right] \\ \sin\left(\frac{M}{H}z\right) t < t_1 \\ p_v + \sum_{m=1}^{\infty}\frac{2}{M}\left[\begin{array}{c}(q_0-p_v)e^{-\beta_m t} + \frac{(q_f-q_0)(e^{-\beta_m (t-t_1)}-e^{-\beta_m t})}{\beta_m t_1} \\ -\frac{1}{\beta_m\overline{B}}\left[\overline{C} + \frac{(-1)^{m+1}p_v(1-k_1)}{M}\right](1-e^{-\beta_m t})\end{array}\right] \\ \sin\left(\frac{M}{H}z\right) t \geqslant t_1 \end{cases} \tag{28}$$

2.3.3. Multistage loading

As shown in Fig. 3c, surcharge preloading is loaded stage by stage when the soil is so soft that it cannot support a large surcharge loading instantaneously. Thus, this method can reduce the risk of the ground failure. For simplicity, the loading is assumed to increase linearly in each stage, which can be expressed as:

$$q(t) = \begin{cases} q_{i-1} + R_i(t - t_{2i-2}) & t_{2i-2} < t < t_{2i-1} \\ q_i & t_{2i-1} < t < t_{2i} \end{cases} (i = 1, 2, 3\cdots)$$
$$R_i = \frac{(q_i - q_{i-1})}{(t_{2i-1} - t_{2i-2})} \tag{29}$$

where i is the ith stage of the loading and qi is the final load of each loading stage.

Substituting Eq. (29) into Eqs. (24b) and (23) leads to:

$$\overline{u}(z,t) = \begin{cases} p_v + \sum_{m=1}^{\infty}\frac{2}{M} \\ \left[\begin{array}{c}(q_0-p_v)e^{-\beta_m t} + \sum_{j=1}^{i-1}\frac{R_j(e^{-\beta_m(t-t_{2j-2})} - e^{-\beta_m(t-t_{2j-1})})}{\beta_m} \\ + \frac{R_i(1-e^{-\beta_m(t-t_{2i-2})})}{\beta_m} \\ -\frac{1}{\beta_m\overline{B}}\left[\overline{C} + \frac{(-1)^{m+1}p_v(1-k_1)}{M}\right](1-e^{-\beta_m t})\end{array}\right] \\ \sin\left(\frac{M}{H}z\right) t_{2i-2} < t < t_{2i-1} \\ p_v + \sum_{m=1}^{\infty}\frac{2}{M} \\ \left[\begin{array}{c}(q_0-p_v)e^{-\beta_m t} + \sum_{j=1}^{i}\frac{R_j(e^{-\beta_m(t-t_{2j-2})} - e^{-\beta_m(t-t_{2j-1})})}{\beta_m} \\ -\frac{1}{\beta_m\overline{B}}\left[\overline{C} + \frac{(-1)^{m+1}p_v(1-k_1)}{M}\right](1-e^{-\beta_m t})\end{array}\right] \\ \sin\left(\frac{M}{H}z\right) t_{2i-1} < t < t_{2i} \end{cases} \tag{30}$$

where j is the summation index of the loading stage.

Using the analytical solution given in above section, the average excess pore water pressure for combined electroosmosis-vacuum-surcharge preloading under three surcharge loading types can be obtained. In addition, when the average excess pore water pressure is obtained, the excess pore water pressure at any place and any time can be calculated by substituting it into Eq. (11), Eq. (9) and Eq. (5a) as:

$$u(r,z,t) = \frac{(A_0 r_e^2 - B_0)}{r_e^2 F_a}[\overline{u} - p(z) + C] + p(z) - \frac{k_e\gamma_w}{k_h}V(r)g(r) \tag{31}$$

2.4. Settlement and degree of consolidation

2.4.1. Settlement

Substituting Eq. (23) into Eq. (17), and then combining with Eq. (2a), the settlement on the surface of soil layer can be expressed as:

$$S = -\int_0^H \frac{\Delta e}{1+e_0}dz = \frac{C_c}{1+e_0}\int_0^H \log\left(1+\frac{q(t)-\bar{u}}{\bar{\sigma}'_0}\right)dz$$
$$= \frac{C_c}{1+e_0}\int_0^H \log\left(1+\frac{q(t)-p_v-\sum_{m=1}^{\infty} e^{-\beta_m t}\left[\int_0^t Q_m(\tau)e^{\beta_m \tau}d\tau+\frac{2(q_0-p_v)}{M}\right]\sin\left(\frac{M}{H}z\right)}{\bar{\sigma}'_0}\right)dz \tag{32}$$

2.4.2. Degree of consolidation

Due to the nonlinear change of soil deformation with the decrease of the excess pore water pressure is considered in this paper, the velocity of the settlement and the dissipation rate of the pore water pressure are different. Using the solution of pore water pressure, the degree of dissipation of pore water pressure can be derived as follows:

$$U_p = \frac{\Delta\bar{\sigma}'}{\Delta\bar{\sigma}'_\infty} = \frac{\int_0^H (q(t)-\bar{u})dz}{\int_0^H (q_f-\bar{u}_\infty)dz} \tag{33}$$

According to Eqs. (26), (28) and (30), the final average excess pore water pressure can be expressed as:

$$\bar{u}_\infty(z) = p_v - \sum_{m=1}^{\infty}\frac{2}{M\bar{B}\beta_m}\left[\bar{C}+\frac{(-1)^{m+1}p_v(1-k_1)}{M}\right]\sin\left(\frac{M}{H}z\right) \tag{34}$$

Following the previous work considering large deformation [17], the degree of consolidation using the change of surface settlement:

$$U_s = \frac{S}{S_\infty} = \frac{\int_0^H \log\left(1+\frac{q(t)-\bar{u}}{\bar{\sigma}'_0}\right)dz}{\int_0^H \log\left(1+\frac{q_f-\bar{u}_\infty}{\bar{\sigma}'_0}\right)dz} \tag{35}$$

Noting that, the integral in Eq. (32) cannot be expressed by elementary functions. Thus, the Newton-Cotes formula [47,48] is used to estimate the value of settlement.

3. Analytical model validation

The proposed analytical model was validated against laboratory tests and numerical results conducted by the Zhou and Deng [29]. In

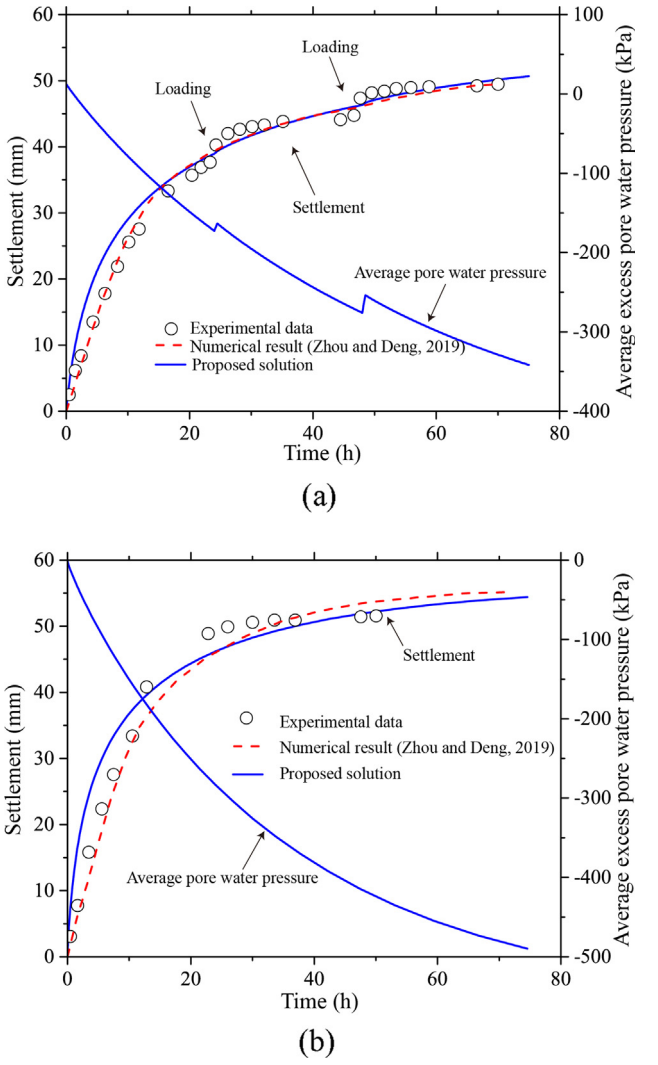

Fig. 4. Development of settlement and average pore water pressure versus time (a) electroosmosis-surcharge preloading; (b) electroosmosis-vacuum preloading.

Table 1
Test soil layer properties and input parameters for analytical model.

Property	Parameters used in two consolidation tests	
	Electroosmosis-surcharge preloading	Electroosmosis-vacuum preloading
Soil thickness H (m)	0.225	0.225
Specific gravity of the solid G_s	2.62	2.62
Initial water content, w_0 (%)	59.4	59.4
Initial void ratio, e_0	1.57	1.57
Compressive index C_c	0.45	0.45
Radial hydraulic permeability index C_{kh}	0.99	0.99
Vertical hydraulic permeability index C_{kv}	0.99	0.99
Electroosmosis permeability index C_{ke}	2.5	2.5
Initial radial hydraulic permeability coefficient k_{h0} ($m{\cdot}s^{-1}$)	2.1×10^{-9}	2.1×10^{-9}
Initial vertical hydraulic permeability coefficient k_{v0} ($m{\cdot}s^{-1}$)	2.1×10^{-9}	2.1×10^{-9}
Initial electroosmosis permeability coefficient k_{e0} ($m^2{\cdot}s^{-1}{\cdot}V^{-1}$)	5.3×10^{-9}	5.3×10^{-9}
Initial effective stress $\bar{\sigma}'_0$(kPa)	20	20
Voltage ϕ_a (V)	20	20
Stage loadings q_i (kPa)	12.5, 25 and 50	0
Vacuum pressure (kPa)	0	−80
Radii of influence zone r_e (m)	0.125	0.125
Radii of smear zone r_s (m)	0.075	0.075
Radii of drain r_w (m)	0.075	0.075

their study, a cylindrical soil chamber (Φ500 × 250 mm in size) with a full-depth cathode sitting in the center and an anode on the periphery of the soil was used. They investigated two test scenarios: electroosmosis-surcharge preloading and electroosmosis-vacuum preloading. The scenario of the electroosmosis-vacuum-surcharge preloading was not studied since the upper cover was not fabricated as expected to work under the simultaneous application of surcharge and vacuum. The material used in their tests was a kaolinite. In the test of electroosmosis-surcharge preloading, the applied voltage was 20 V with a potential gradient 170 V/m. The surcharge loadings were applied incrementally in three stages, t = 0, 24 and 48 h. In the test of electroosmosis-vacuum preloading, the voltage gradient remained as 170 V/m. A vacuum pressure of −80 kPa was applied throughout the test. This pressure was assumed to remain constant in the cathode drain due to the relatively shallow depth of the vertical drain. During the tests, a dial gauge was mounted to the rigid loading cap to record the average soil settlement. The soil properties, load details and model parameters were taken from literature [29], which are shown in Table 1.

The experimental measured settlement and numerical and analytical results for the two scenarios are presented in Fig. 4. In Fig. 4a, the results include the settlement and average pore water pressure versus time for the soil layer subjected to the combined usage of voltage and surcharge loads. The final settlement is up to 50 mm (22.2% strain), which means the nonlinear changes of soil parameter induced by the large soil deformation are necessary to be considered. It can be found that the settlement obtained using analytical solution agrees well with the experimental and numerical results. Besides, according to the result of average pore water pressure obtained by the analytical solution, it also indicates that the proposed analytical model can satisfactorily capture the jumps associated with the stepped loading. Even so, there is also a little difference between the analytical solution and experimental result within the first 20 h. The analytically predicted settlement is slightly larger than that of experimental observation and numerical solution at the beginning of the test, and this difference becomes increasing small with the time. This can be attributed to the simplified approach by replacing $\overline{\sigma}'/\overline{\sigma}'_0$ with the approximation $[\overline{\sigma}'_0 + \overline{\sigma}'_{t=+\infty}]/2\overline{\sigma}'_0$ in the derivation of analytical solution. Using this simplification, the soil compressibility coefficient is smaller than its practical value at the beginning of the test, which accelerates the dissipation rate of the excess pore water pressure and leads to the faster settlement. Despite the simplification, the predicted results from the analytical solution are still consistent with the experimental data and numerical solutions in general. Similarly, a good agreement is also attained in Fig. 4b, which presents the settlement versus time for the test of electroosmosis-vacuum preloading. Therefore, given the results of agreement in the two tests, the capability of the proposed analytical model with consideration of nonlinearity is proved to be effective in predicting consolidation of combined electroosmosis-vacuum-surcharge preloading.

Fig. 5 presents the development of degrees of consolidation and dissipation versus time for the two scenarios. It can be found that the consolidation rate of settlement (U_s) is remarkably faster than that of dissipation rate of pore water pressure (U_p), which is greatly attributed to the nonlinear changes of the soil deformation with the increases of effective stress. Thus, if the degree of dissipation of pore water pressure U_p is chosen as the design index, the construction time will be prolonged and leads to the increase of construction cost. Actually, water flow is the main factor that governed the consolidation process in the saturated soils. Considering the water discharge and settlement are two preferred measurements of the consolidation in the field projects, and the water discharge changes linearly with the settlement when the soil layer is highly saturated, the degree of consolidation U_s is more suitable to be chosen as the design parameter. This is the same as that in case of consolidation considering large deformation [29,38]. Thus, the degree of consolidation U_s is used in the next analysis.

4. Parametric study

To study the effect of nonlinear variation of soil parameters on the consolidation behavior under combined electroosmosis-vacuum-surcharge preloading, parameter analyses were conducted using the proposed analytical solutions. The basic parameters used in the analytical model are presented in Table 2. The ground and EVD installations were determined in terms of field applications. The value ranges used in the table define a medium thick, saturated, high compressibility clay layer.

In the analysis, the pore water pressure is the average value in different depth and radius, which is defined as:

$$\overline{u}_{rz} = \frac{\int_0^H \overline{u}(z, t)dz}{H} \tag{36}$$

4.1. Effect of considering nonlinearity

In this subsection, the analytical solution without considering nonlinearity for combined electroosmosis-vacuum-surcharge preloading consolidation [24] was adopted as comparison to illustrate the advantage of the proposed analytical solution with the consideration of nonlinearity.

Fig. 6 shows the influence of the compressibility index C_c on the consolidation process. In this analysis, the single-stage loading was adopted with the loading rate 60 kPa per day within the initial 5 days. The compressibility index was chosen as 0.3, 0.5 and 0.7, respectively, while the other parameters were kept as those in Table 2. It needs to point out that compressibility index C_c was transferred into initial compressibility coefficient m_{v0} using the relation shown in Eq. (15) when it used in the solution without considering nonlinearity. Since the larger compressibility index of the soft soil leads to the lower the modulus of compressibility and the larger deformation. It can be observed in Fig. 6a that an increase of compressibility index leads to the larger excess pore water pressure in the first loading stage and slows down the dissipation of the pore water pressure after that. However, the dissipation of the pore water pressure is faster with the consideration of nonlinear deformation than that without considering nonlinearity. This can be explained by the decrease of the compressibility coefficient with the increase of effective stress with the consideration of nonlinear. Thus, the influence of the compressibility index on the development of excess pore water pressure varies. For instance, the difference of the development of pore water pressure with and without considering nonlinearity becomes remarkable in the first loading stage for the soils with the smaller compressibility index, for the excess pore water pressure in the loading stage becomes much smaller with the consideration of nonlinearity. This is mainly attributed to the obviously increase of

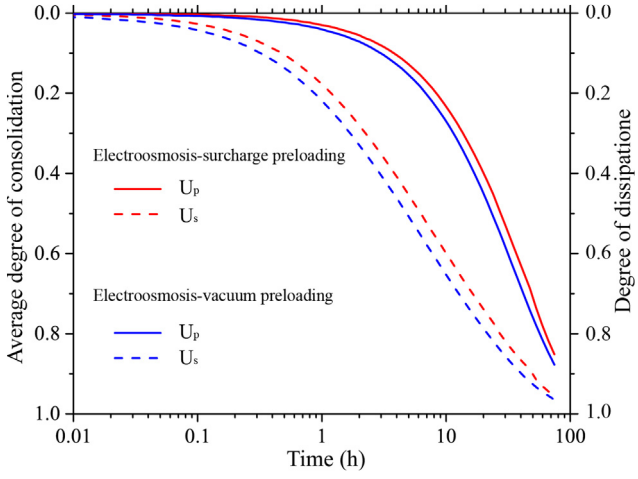

Fig. 5. Development of degrees of consolidation and dissipation versus time.

Table 2
Basic soil layer properties and analytical model input parameters.

Property	Value
Soil thickness H (m)	5.0
Specific gravity of the solid G_s	2.65
Initial void ratio, e_0	2.1
Compressive index C_c	0.5
Radial hydraulic permeability index C_{kh}	1.0
Vertical hydraulic permeability index C_{kv}	1.0
Electroosmosis permeability index C_{ke}	2.5
Initial radial hydraulic permeability coefficient k_{h0} ($m{\cdot}s^{-1}$)	2×10^{-9}
Initial vertical hydraulic permeability coefficient k_{v0} ($m{\cdot}s^{-1}$)	2×10^{-9}
Initial electroosmosis permeability coefficient k_{e0} ($m^2{\cdot}s^{-1}{\cdot}V^{-1}$)	2×10^{-9}
Initial effective stress $\bar{\sigma}'_0$ (kPa)	50
Voltage ϕ_a (V)	30
Initial surcharge loadings q_0 (kPa)	0
Final surcharge loadings q_f (kPa)	300
Vacuum pressure p_v (kPa)	−80
Reduction factor of vacuum pressure along the drains k_1	0.5
Radii of influence zone r_e (m)	1.0
Radii of smear zone r_s (m)	0.15
Radii of drain r_w (m)	0.05
Ratio of radial hydraulic permeability coefficients in smear zone η_1	2.0
Ratio of radial electroosmosis permeability coefficients in smear zone η_2	1.0

the soil compressibility modulus, which then will quicken the development of negative pore water pressure under electroosmosis and vacuum preloading. Additionally, due to the nonlinear change of hydraulic and electroosmosis permeability with the soil deformation as expressed by Eqs. (2b) to (2d), the value of k_e/k_h governing the final excess pore water pressure changes during the electroosmosis consolidation process. Since the decrease of electroosmosis permeability with the decrease of void ratio is smaller than that of hydraulic permeability, the value of k_e/k_h is larger for soils with the higher compressibility, which leads to the larger final negative pore water pressure. In contrast, for analytical solution without considering nonlinearity, the pore water pressures for different compressibility coefficient approach the same final value. Fig. 6b shows that the development of consolidation can be accelerated with the consideration of nonlinear vary of soil parameters. Thus, the influence of the soil compressibility on the consolidation process is larger compared with that without considering nonlinearity from above analysis.

Fig. 7 compares the influence of the applied voltage on the consolidation behavior with and without considering nonlinearity. In this analysis, the single-stage loading was applied which is the same as introduced above, the applied voltage was set as 10, 30 and 50 V with the other parameters kept as the same as those in Table 2. It can be investigated that the influence of the applied voltage varies with the consideration of nonlinear change of soil parameters. As shown in Fig. 7a, the applied voltage has a limited influence on the generation of the excess pore water pressure during loading stage when ignoring the nonlinearity. However, the peak value of the excess pore water pressure after loading decreases obviously with the larger applied voltage when considering the nonlinear change of soil parameters. This can be explained by the fact that the value of k_e/k_h increases remarkably with the soil deformation, which magnifies the effects of applied voltage to produce negative pore water pressure, and improves the generation of the larger soil deformation in turn. After loading, the excess pore water pressure dissipates with time under combined electroosmosis and vacuum preloading, and the dissipation of the pore water pressure is obviously faster with the consideration of nonlinearity. It is worth to note that the difference of pore water pressure between considering and without considering nonlinearity increases with the increase of applied voltage, which caused by the larger soil deformation with the higher applied voltage and increasing the value of k_e/k_h in return. Fig. 7b shows the development of average degree of consolidation under three different applied voltages. It can be found that the applied voltage has a

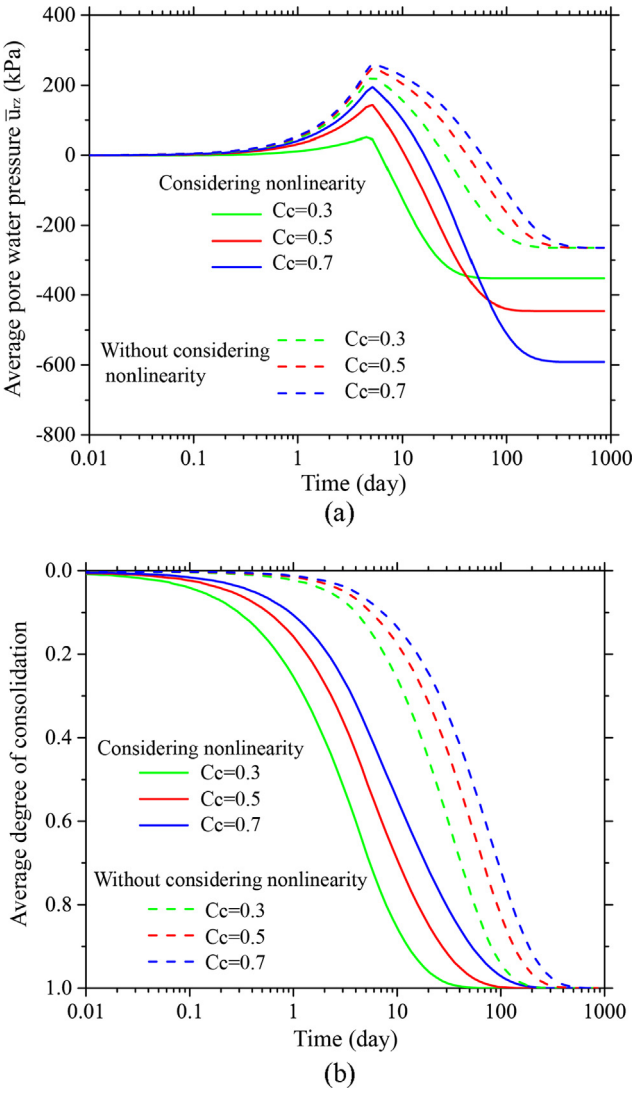

Fig. 6. Effect of compressibility index on the (a) dissipation of pore water pressure and (b) development of degree of consolidation with and without considering nonlinearity.

negligible influence on the consolidation rate when ignoring the nonlinearity. However, with the consideration of nonlinearity, the consolidation time can be effectively shortened with the larger applied voltage, which is consistent with the laboratory observation [43].

The development of the pore water pressure and degree of consolidation for different loading process is shown in Fig. 8 to investigate the effect of considering nonlinearity. It is also shown that considering nonlinearity can predict the faster dissipation of the pore water pressure and the larger final negative pore water pressure no matter what the patterns of surcharge loading applied. In Fig. 8a, it is easy to see that the maximum excess pore water pressure decreases with gradual surcharge loading applied, especially for the case considering nonlinear deformation, which was also given in previous literature considering combined vacuum and surcharge preloading [44]. In addition, with the combined action of electroosmosis, the stability of soft foundation under the surcharge loading can be approved for the loading-induced positive excess pore water pressure can be effectively counteracted by the electroosmosis-induced negative pore water pressure. For both analytical solutions with and without considering nonlinearity, the same final pore water pressures are arrived for three patterns of surcharge loading, which means no influence of surcharge loading type on the final improvement effect. As shown in Fig. 8b, the consolidation

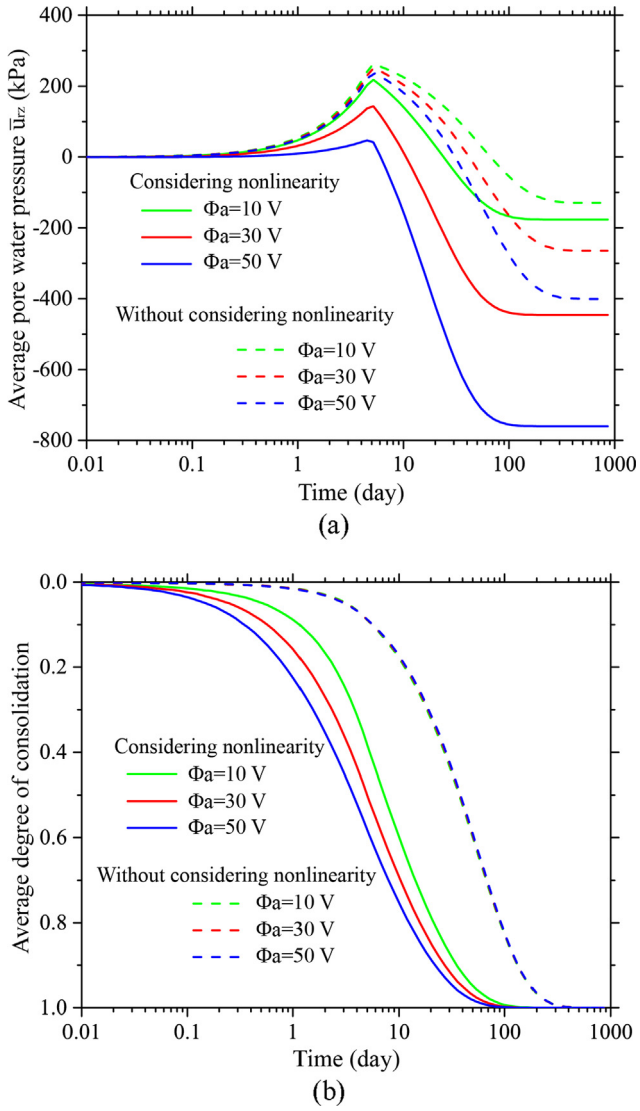

Fig. 7. Effect of applied voltage on the (a) dissipation of pore water pressure and (b) development of degree of consolidation with and without considering nonlinearity.

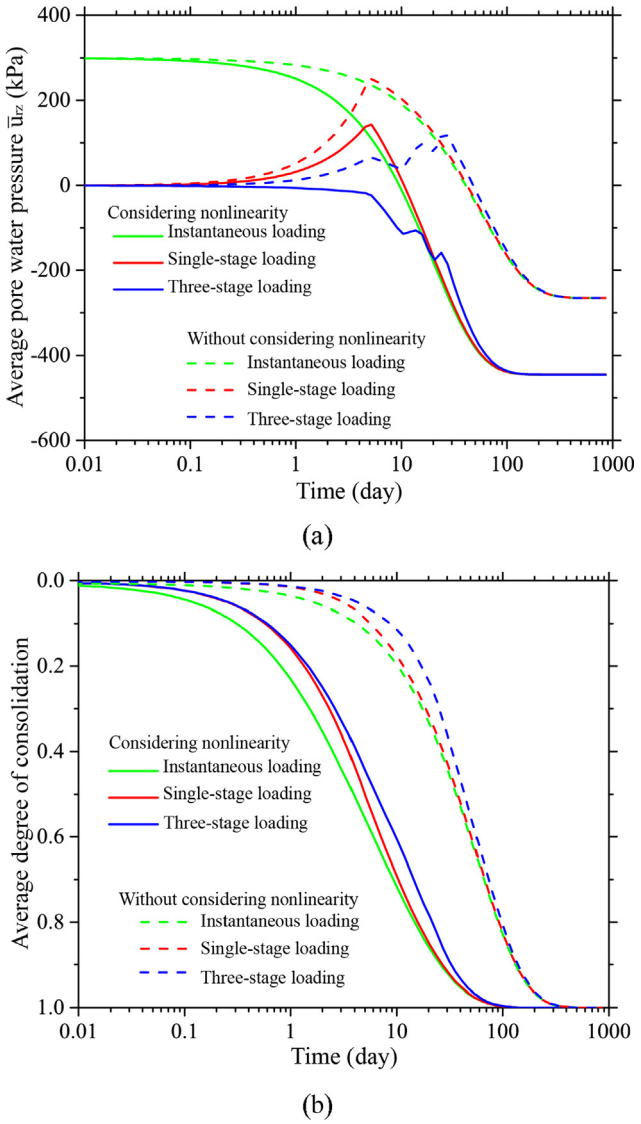

Fig. 8. Effect of loading type on the (a) dissipation of pore water pressure and (b) development of degree of consolidation with and without considering nonlinearity.

time can also be remarkable shortened with the consideration of nonlinearity for three patterns of surcharge loading, and the time arriving the final consolidation are the same with each other.

4.2. Effect of smear zone

To gain a further insight into the consolidation efficiency, the influence of the smear zone on the consolidation behaviour was examined using the proposed analytical solution. As introduced in the previous studies, a smear zone varies in diameter and hydraulic permeability depending on the mandrel size and soil type [45,46]. The normal ranges are up to four times the drain diameter and as low as one half of the hydraulic permeability of the native soil. Therefore, the effects of the smear zone size and reduction of hydraulic permeability in the smear zone are need to be investigated in the design. In this study, the instantaneously loading was adopted, the parameters used in the analytical solution was the same as those in Table 2. The effect of smear zone size on the consolidation behaviour was studied first with the diameter chosen as r_s/r_w = 1.0, 3.0 and 7.0 and the hydraulic permeability coefficient of the smear zone fixed as $0.5k_h$ (η_1 = 2). It needs to point out that the value of r_s/r_w = 1 means the case where there is no smear zone. The results of average pore water pressure, degree of

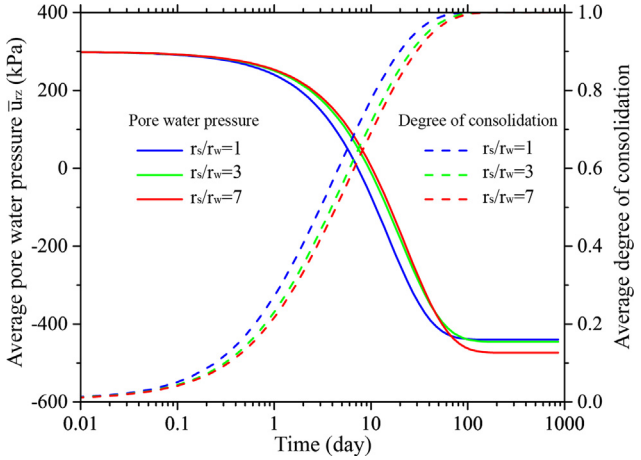

Fig. 9. Effect of smear zone size on the average pore water pressure and degree of consolidation under combined electroosmosis-vacuum-surcharge preloading.

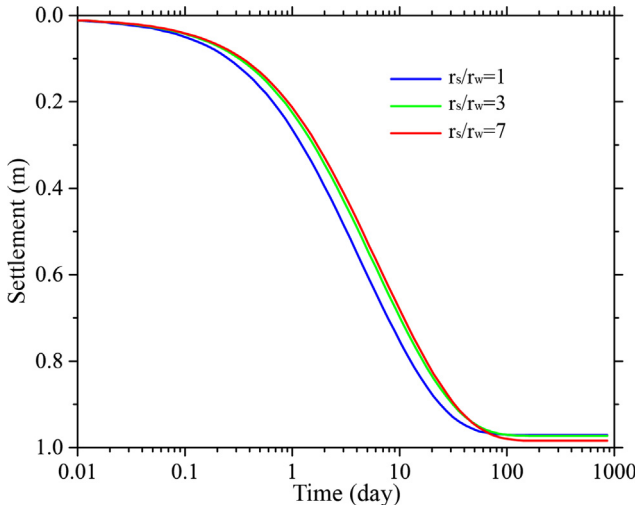

Fig. 10. Effect of smear zone size on the settlement under combined electro-osmosis-vacuum-surcharge preloading.

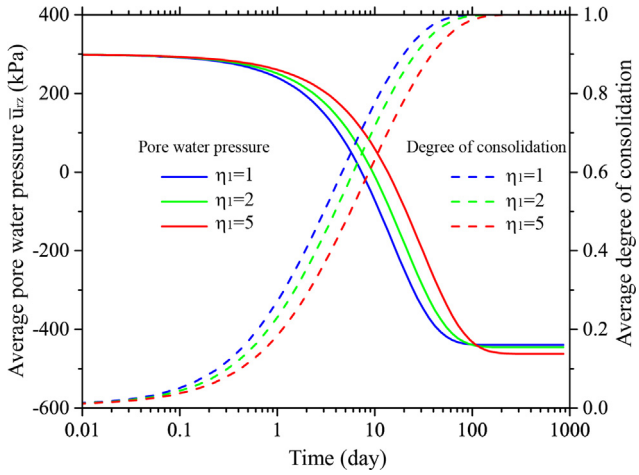

Fig. 11. Effect of hydraulic permeability in smear zone on the average pore water pressure and degree of consolidation under combined electroosmosis-vacuum-surcharge preloading.

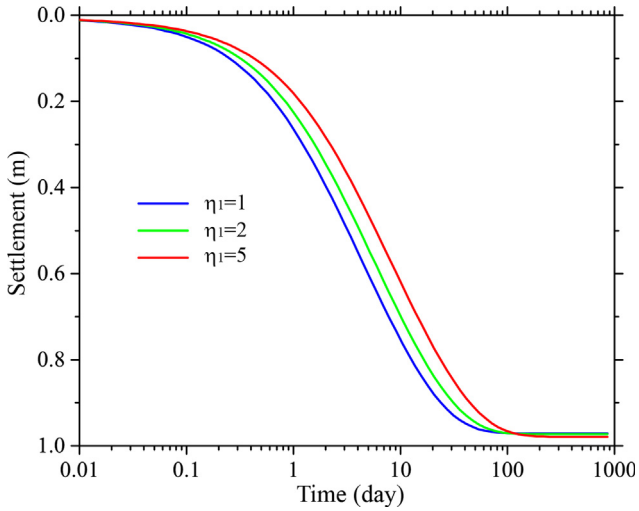

Fig. 12. Effect of hydraulic permeability in smear zone on the settlement under combined electroosmosis-vacuum-surcharge preloading.

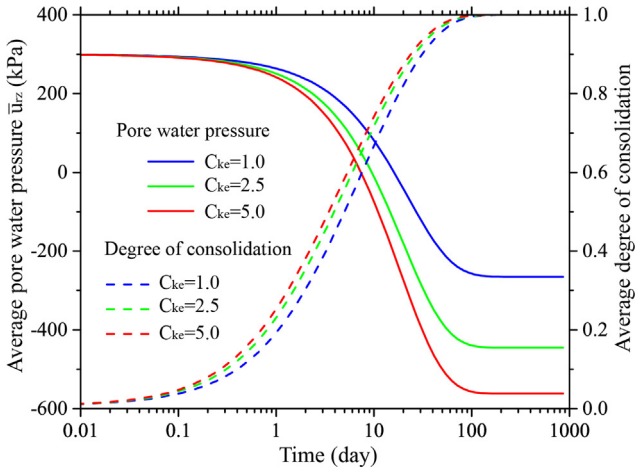

Fig. 13. Effect of C_{ke} on the average pore water pressure and degree of consolidation under combined electroosmosis-vacuum-surcharge preloading.

consolidation and settlement are given in Figs. 9 and 10. Compared with the case without smear zone, the consolidation progress is significantly delayed with the appearance of smear zone. Meanwhile, the final negative pore water pressure and settlement increase marginally with the increase of smear zone diameter. This can be explained by the increase of average value of k_e/k_h in the soil layer, which governing the final negative pore water pressure, with the increase of smear zone diameter. In addition, the curves of the degree of consolidation for the two smeared cases remain close, which means a little influence of the smear zone diameter on the consolidation rate under combined electroosmosis-vacuum-surcharge preloading. Secondly, the effect of the hydraulic permeability coefficient in the smear zone was investigated with the values η_1 selected as 1.0, 2.0 and 5.0 and the diameter of smear zone fixed as $3.0r_w$. Noting that, the value of $\eta_1 = 1$ is corresponding to the case without considering smear effect. The analytical results are presented in Figs. 11 and 12. The final average negative pore water pressure and settlement increase with the decrease of hydraulic permeability in the smear zone. Meanwhile, the less permeable the smear zone is, the smaller the degree of consolidation in the soil layer. These results mean that the permeability of the smear zone inversely influences the settlement and positively influences the degree of consolidation if the other conditions kept constant. To our satisfactory, above results obtained by the analytical model were also found by the numerical simulation considering the large deformation [29], which

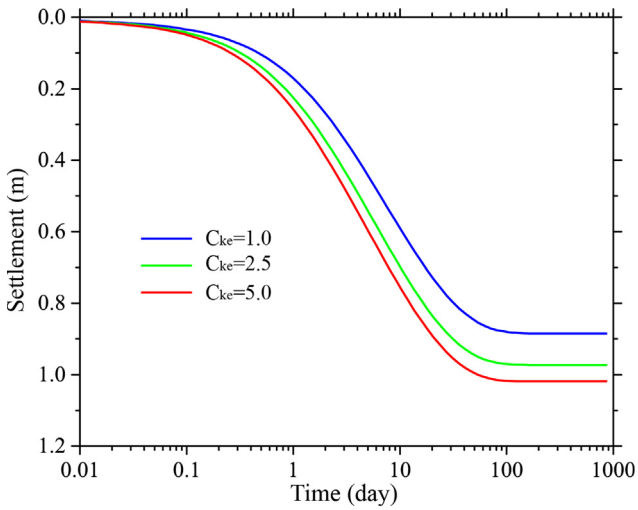

Fig. 14. Effect of C_{ke} on the settlement under combined electroosmosis-vacuum-surcharge preloading.

confirms the reliability of the proposed analytical solution with the consideration of nonlinearity.

4.3. Effect of C_{ke}

Since the non-synchronous variations of hydraulic permeability and electroosmosis permeability with the soil deformation, the nonlinear consolidation behavior in the case of combined electroosmosis-vacuum-surcharge preloading is also affected by the ratio of the electroosmosis permeability index to the hydraulic permeability index. Considering the change of electroosmosis permeability with the void ratio is smaller than that of hydraulic permeability in practice, the value of C_{ke} was chosen as 1.0, 2.5 and 5.0, respectively, while the value of C_{kh} was kept as 1.0. Note that, when the ratio of C_{ke}/C_{kh} is equal to 1.0, the changes of hydraulic permeability and electroosmosis permeability are synchronous, which means the value of k_e/k_h keeps constant in the consolidation process. Figs. 13 and 14 show the influence of the electroosmosis permeability index C_{ke} on the average pore water pressure, degree of consolidation and settlement. The average pore water pressure is greatly affected by the value of C_{ke}/C_{kh}, with the final pore water pressures for the values of C_{ke}/C_{kh} 1.0, 2.5 and 5.0 are −265.1 kPa, −445.3 kPa and −561.7 kPa, respectively. The maximum difference of pore water pressure reaches about 300 kPa. Moreover, a larger value of C_{ke} gives the larger degrees of consolidation because a high value of C_{ke} implies a smaller decrease of electroosmosis permeability with the soil compression deformation. It can also notice that the difference of average degree of consolidation decreases with the increasing C_{ke}, which indicates the influence of the electroosmosis permeability index on the consolidation rate becomes increasingly small with an increase in the value of C_{ke}/C_{kh}. In Fig. 14, the average settlement increases with the increase in electroosmosis permeability index where the hydraulic permeability index is fixed. The settlement values are 0.89, 0.97 and 1.02 m, which is corresponding to the values of C_{ke}/C_{kh} 1.0, 2.5 and 5.0. A decreasing difference of the settlement with the increasing electroosmosis permeability index can be found. Therefore, the effect of electroosmosis permeability index can be ignored where there is a large value of C_{ke}/C_{kh} for the treated soils from a practical standpoint, such as 5.0 in this analysis.

4.4. Effect of C_{kv}

Figs. 15 and 16 present the variations in the average pore water pressure, degree of consolidation and settlement versus time under different value of C_{kv}. In this comparison, the surcharge loading was assumed to be applied instantaneously, the value of C_{kv} was chosen as 0.1, 1.0 and 5.0, while the other parameters were the same as those in Table 2. Noting that, when the value of C_{kv} is equal to 1.0, the change of the vertical hydraulic permeability with the void ratio is the same as that of horizontal hydraulic permeability. While the value of C_{kv} is larger than 1.0, the decrease of the vertical hydraulic permeability is smaller, and the value of C_{kv} is smaller than 1.0, the decrease of the vertical hydraulic permeability is larger. It can be found that the ultimate negative pore water pressure and settlement increase with the decrease of C_{kv}, but the consolidation time is prolonged. From Eq. (2c), when the value of C_{kv} is approached to the infinitely small, a slight decrease of void ratio will induce the significant decrease of vertical hydraulic permeability, and leading to the case of without considering vertical flow. Thus, without consideration of vertical flow or overestimating of the decrease of vertical hydraulic permeability will induced the overestimate of the final settlement and consolidation time.

5. Conclusion

This paper derives an analytical solution for the nonlinear consolidation with coupled radial-vertical flow under combined electroosmosis-vacuum-surcharge preloading, by considering the depth-dependent vacuum pressure, the variation of soil compressibility hydraulic permeability and electroosmosis permeability with void ratio. Then, detailed solutions are provided for instantaneous, single-stage, and multistage loading. The present solution is verified by compared with experimental and numerical results of settlement in a previous study. Finally, the nonlinear consolidation behaviour is investigated using the parametric analysis, and the results show that:

1. With the consideration of nonlinearity, the consolidation process is accelerated compared with that without considering nonlinearity, and the influence of the soil compressibility becomes more obvious. The result shows a significant delay of the consolidation process and an increase of the final negative pore water pressure with the increase of compressibility index with the consideration of nonlinearity.
2. The influence of the applied voltage on the consideration behaviour is magnified with the consideration of nonlinearity. The increase of the final negative pore water pressure with the increasing applied voltage becomes more remarkable, and the difference of the degree of consolidation for various applied voltage can be well reflected.
3. Application of multistage surcharge loading combined with electroosmosis and vacuum pressure can effectively reduce the excess pore water pressure generated in the loading process, especially for the case considering the nonlinear change of the soil parameters with void ratio.
4. The presence of a smear zone delays the progress of consolidation and increases the final negative pore water pressure and settlement, and this effect increases with the increase of smear zone range and decrease of hydraulic permeability coefficient of the smear zone, with the consideration of nonlinearity.
5. The ratio of the electroosmosis permeability index to the hydraulic permeability index (C_{ke}/C_{kh}) significantly affect consolidation process. With an increase in the value of C_{ke} where the value of C_{kh} is kept constant, the final negative pore water pressure, settlement and consolidation rate are increased, but the further increases are limited with the continue increasing value of C_{ke}/C_{kh}.
6. With a decrease in the value of C_{kv}, the final negative pore water pressure, settlement and consolidation time are increased, and it is the same as the case of without considering vertical flow when the value of C_{kv} approaches infinitely small.

CRediT authorship contribution statement

Liujiang Wang: Conceptualization, Methodology, Software, Formal analysis, Supervision. **Penghua Huang:** Software, Validation, Writing -

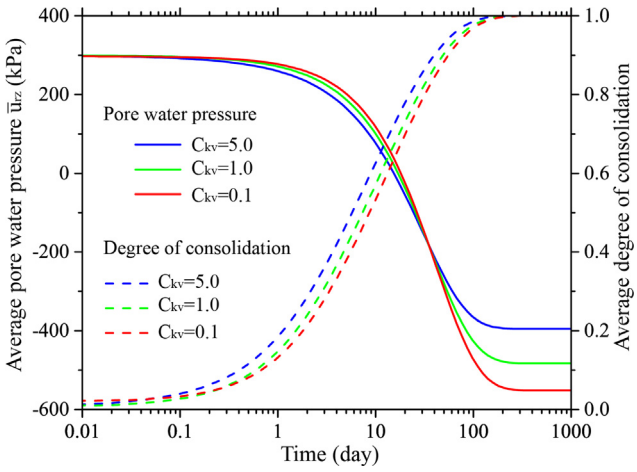

Fig. 15. Effect of C_{kv} on the average pore water pressure and degree of consolidation under combined electroosmosis-vacuum-surcharge preloading.

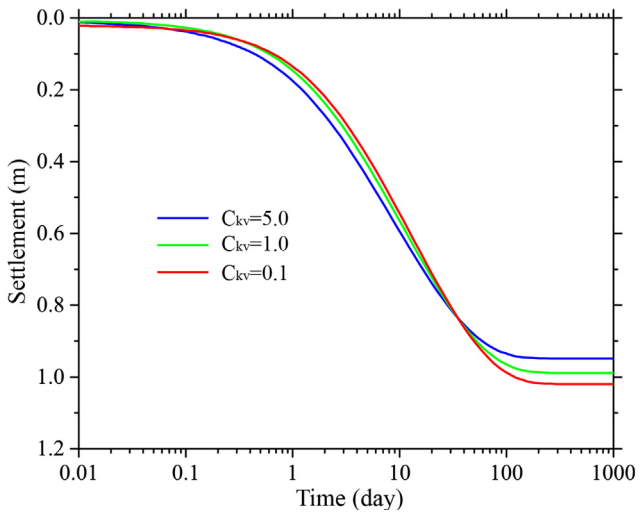

Fig. 16. Effect of C_{kv} on the settlement under combined electroosmosis-vacuum-surcharge preloading.

original draft. **Sihong Liu:** Formal analysis, Writing - review & editing.

Eduardo Alonso: Formal analysis, Writing - review & editing.

Declaration of Competing Interest

The authors declare that they have no known competing financial interests or personal relationships that could have appeared to influence the work reported in this paper.

Acknowledgments

The authors greatly appreciate the financial support from the Fundamental Research Funds for the Central Universities (Project No. 2019B11214) and the Joint Funds of the National Natural Science Foundation of China (U1765205). The first author is grateful for the financial support from the China Scholarship Council (CSC) (201806715020) for his joint research at UPC, Barcelona Tech. Finally, we thank the reviewers and the editor for their excellent comments and suggestions to improve the quality of this paper.

Appendix A

When the time approaches infinite for electroosmosis consolidation, the following equation can be satisfied for the pore water flow in the radio direction:

$$\frac{k_h f_1(r)}{\gamma_w}\frac{\partial u_{eo}^{ult}}{\partial r} + k_e f_2(r)\frac{\partial V(r)}{\partial r} = 0 \tag{A1}$$

Thus:

$$\frac{\partial u_{eo}^{ult}}{\partial r} = -\frac{k_e \gamma_w}{k_h}\frac{\partial V(r)}{\partial r} g(r) \tag{A2}$$

Considering the nonlinear change of hydraulic and electroosmosis permeabilities according Eqs. (2a), (2b), and (2d):

$$k_h = k_{h0}\left(\frac{\bar{\sigma}'}{\bar{\sigma}'_0}\right)^{-\frac{C_c}{C_{kh}}}$$
$$k_e = k_{e0}\left(\frac{\bar{\sigma}'}{\bar{\sigma}'_0}\right)^{-\frac{C_c}{C_{ke}}} \tag{A3}$$

Taking Eq. (A3) into (A2) leads to the following equation:

$$\frac{\partial u_{eo}^{ult}}{\left(\frac{\bar{\sigma}'_{ult}}{\bar{\sigma}'_0}\right)^{-\frac{C_c}{C_{ke}}+\frac{C_c}{C_{kh}}}} = -\frac{k_{e0}\gamma_w}{k_{h0}}\frac{\partial V(r)}{\partial r} g(r)dr \tag{A4}$$

Defining:

$$\bar{\sigma}'_{ult}(r) = \bar{\sigma}'_0 + q_f - \frac{1}{2}p_v(1+k_1) - u_{eo}^{ult} \tag{A5}$$

Then, Eq. (A4) can be transferred into:

$$\frac{\partial u_{eo}^{ult}}{(a - b u_{eo}^{ult})^n} = -\frac{k_{e0}\gamma_w}{k_{h0}}\frac{\partial V(r)}{\partial r} g(r)dr \tag{A6}$$

where

$$\text{a} = \left[\bar{\sigma}'_0 + q_f - \frac{1}{2}p_f(1+k_1)\right] \Big/ \bar{\sigma}'_0 \tag{A7}$$

$$\text{b} = 1/\bar{\sigma}'_0 \tag{A8}$$

$$\text{n} = -\frac{C_c}{C_{ke}} + \frac{C_c}{C_{kh}} \tag{A9}$$

Integrating Eq. (A6), the solution of final pore water pressure induced by electroosmosis in the radial direction is given as:

$$u_{eo}^{ult} = \frac{a}{b} - \left\{ \frac{(1-n)bk_{e0}\gamma_w}{k_{h0}} V(r)g(r) + a^{1-n} \right\}^{\frac{1}{1-n}} \Big/ b \tag{A10}$$

Then, the average final pore water pressure induced by electroosmosis can be

$$\overline{u}_{eo}^{ult} = \frac{1}{\pi(r_e^2 - r_w^2)} \int_{r_w}^{r_e} 2\pi r u_{eo}^{ult}(r) dr \tag{A11}$$

The integration of Eq. (A11) can be obtained using the numerical method of Newton-Cotes formula.

References

[1] Chu J, Yan SW, Yang H. Soil improvement by the vacuum preloading method for an oil storage station. Géotechnique 2000;50(6):625–32.
[2] Mohamedelhassan E, Shang JQ. Vacuum and surcharge combined one-dimensional consolidation of clay soils. Can Geotech J 2002;39(5). 1126–1138(13).
[3] Zhuang Y, Cui XY. Evaluation of vacuum preloading with vertical drains as a soft soil improvement measure. Soil Mech Found Eng 2016;53(3):210–7.
[4] Geng X, Yu HS. A large-strain radial consolidation theory for soft clays improved by vertical drains. Géotechnique 2017;67(11):1020–8.
[5] Zhou WH, Lok MH, Zhao LS, Mei GX, Li XB. Analytical solutions to the axisymmetric consolidation of a multi-layer soil system under surcharge combined with vacuum preloading. Geotext Geomembr 2017;45(5):487–98.
[6] Hansbo S. Consolidation of fine-grained soils by prefabricated drains. Procof ICSMFE 1980;3:677–82.
[7] Chai JC, Hong ZS, Shen SL. Vacuum-drain consolidation induced pressure distribution and ground deformation. Geotext Geomembr 2010;28(6):525–35.
[8] Geng XY, Indraratna B, Rujikiatkamjorn C. Analytical solutions for a single vertical drain with vacuum and time-dependent surcharge preloading in membrane and membraneless systems. Int J Geomech 2010;10(1):27–42.
[9] Griffin H, Okelly BC. Ground improvement by vacuum consolidation-a review. Procee Institution Civil Engineers: Ground Improve 2014;167(4):274–90.
[10] Ni PP, Xu K, Mei GX, Zhao YL. Effect of vacuum removal on consolidation settlement under a combined vacuum and surcharge preloading. Geotext Geomembr 2019;47(1):12–22.
[11] Wang J, Ma JJ, Liu FY, Mi W, Cai YQ, Fu HT. Experimental study on the improvement of marine clay slurry by -vacuum preloading. Geotext Geomembr 2016;44(4):615–22.
[12] Shi L, Wang QQ, Xu SL, Pan XD, Sun HL, Cai YQ. Numerical study on clogging of prefabricated vertical drain in slurry under vacuum loading. Granul Matter 2018;20(4):74.
[13] Rujikiatkmajorn C. Physical modelling of soft clay consolidation using vacuum-surcharge method. Aust Geomech J 2012;47(3):27–34.
[14] Liu HL, Cui YL, Shen Y, Ding XM. A new method of combination of, vacuum and surcharge preloading for soft ground improvement. China Ocean Eng 2014;28(4):511–28.
[15] Casagrande L. Stabilization of soils by means of electro-osmotic-state-of-art. J Boston Civ Eng ASCE 1983;69:255–302.
[16] Peng J, Xiong X, Mahfouz AH, Song ER. Vacuum preloading combined electro-osmosis strengthening of ultra-soft soil. J Central South Univ 2013;20(11):3282–95.
[17] Deng A, Zhou YD. Modeling and surcharge preloading consolidation II: validation and simulation results. J Geotech Geoenviron 2016;142(4):04015094.
[18] Wan TY, Mitchell JK. Electro-osmotic consolidation of soils. J Geotech Eng Div 1976;102(5):473–91.
[19] Shang JQ. enhanced preloading consolidation via vertical drains. Can Geotech J 1998;35(3):491–9.
[20] Hu LM, Wu WL, Wu H. Numerical model of electro-osmotic consolidation in clay. Geotechnique 2012;62(6):537–41.
[21] Wu H, Hu LM. Analytical solution for axisymmetric electro-osmotic consolidation. Géotechnique 2013;63(12):1074–9.
[22] Xu W, Liu SH, Wang LJ, Wang JB. Analytical theory of soft ground consolidation under vacuum preloading combined with electro-osmosis. J Hohai Univ (Nat Sci) 2011;30(2):169–75. [in Chinese].
[23] Wang LJ, Wang YM, Liu SH, Yuan J. 2D analytical solution of consolidation for vacuum preloading combined with electro-osmosis drainage considering reduction of effective voltage. Chinese J Rock Mech Eng 2019;38(S1):3134–41. [in Chinese].
[24] Wang LJ, Wang YM, Liu SH, Xue CY. Analytical solution to the axisymmetric consolidation under surcharge-vacuum-. Environ Geotech 2019:1–12.
[25] Townsend FC, Mcvay MC. SOA: large strain consolidation predictions. J Geotech Eng-ASCE 1990;116(2):222–43.
[26] Feldkamp JR. Numerical-analysis of one-dimensional nonlinear large-strain consolidation by the finite-element method. Transport Porous Med 1989;4(3):239–57.
[27] Yuan J, Hicks MA. Large deformation elastic electro-osmosis consolidation of clays. Comput Geotech 2013;54:60–8.
[28] Zhou YD, Deng A, Wang C. Finite-difference model for one-dimensional electro-osmotic consolidation. Comput Geotech 2013;54:152–65.
[29] Zhou YD, Deng A. Modelling combined electroosmosis-vacuum-surcharge preloading consolidation considering large-scale deformation. Comput Geotech 2019;109:46–57.
[30] Deng A, Zhou YD. Modeling and surcharge preloading consolidation. I: model formulation. J Geotech Geoenviron 2016;142(4):04015093.
[31] Wang LJ, Liu SH, Wang ZJ, Zhang K. A consolidation theory for one-dimensional large deformation problems under combined action of load and electroosmosis. Eng Mech 2013;30(12):91–8. [in Chinese].
[32] Gibson RE, Schiffman RL, Cargill KW. The theory of one-dimensional consolidation of saturated clays. 2. Finite non-linear consolidation of thick homogeneous layers. Can Geotech J 1981;18(2):280–93.
[33] Wu H, Qi WG, Hu LM, Wen QB. Electro-osmotic consolidation of soil with variable compressibility, hydraulic conductivity and electro-osmosis conductivity. Comput Geotech 2017;85:126–38.
[34] Wang LJ, Wang YM, Liu SH, Fu ZZ, Shen CM, Yuan WH. Analytical solution for one-dimensional vertical electro-osmotic drainage under unsaturated conditions. Comput Geotech 2019;105:27–36.
[35] Lekha KR, Krishnaswamy NR, Basak P. Consolidation of clay by sand drain under time-dependent loading. J Geotech Geoenviron Eng 1998;124(1):91–4.
[36] Indraratna B, Rujikiatkamjorn C, Sathananthan I. Analytical and numerical solutions for a single vertical drain including the effects of vacuum preloading. Can Geotech J 2005;42(4):994–1014.
[37] Lu M, Wang S, Sloan SW, Sheng D, Xie K. Nonlinear consolidation of vertical drains with coupled radial-vertical flow considering well resistance. Geotext Geomembr 2015;43(2):182–9.
[38] Barron RA. Consolidation of fine-grained soils by drain wells. Trans Am Soc Civ Eng 1948;113:718–42.
[39] Esrig MI. Pore pressures, consolidation and electro-kinetics. J Soil Mech Found Engng Div ASCE 1968;94(4):899–921.
[40] Indraratna B, Bamunawita C, Khabbaz H. Numerical modeling of vacuum preloading and field applications. Can Geotech J 2004;41(6):1098–110.
[41] Xie KH, Lu MM, Liu GB. Equal strain consolidation for stone columns reinforced foundation. Int J Numeric Analytic Meth Geomech 2010;33(15):1721–35.
[42] Tang X, Onitsuka K. Consolidation by vertical drains under time-dependent loading. Int J Numeric Analytic Meth Geomech 2000;24(9):739–51.
[43] Li Y, Gong XN, Zhang XC. Experimental research on effect of applied voltage on one-dimensional electroosmosis drainage. Rock and Soil Mech 2011;32(3):709–14. [in Chinese].
[44] Liu S, Geng X, Sun H, Cai Y, Pan X, Shi L. Nonlinear consolidation of vertical drains with coupled radial-vertical flow considering time and depth dependent vacuum pressure. Int J Numer Anal Methods Geomech 2019;43:767–80.
[45] Hansbo S. Consolidation by vertical drains. Geotechnique 1981;31(1):45–66.
[46] Sathananthan I, Indraratna B. Laboratory evaluation of smear zone and correlation between permeability and moisture content. J Geotech Geoenviron 2006;132(7):942–5.
[47] Kalogiratoua Z, Simosb TE. Newton-Cotes formulae for long-time integration. J Comput Appl Mathem 2003;158:75–82.
[48] Zhao H, Jiang K, Yang R, Tang Y, Liu J. Experimental and theoretical analysis on coupled effect of hydration, temperature and humidity in early-age cement-based materials. Int J Heat Mass Transfer 2020;146:118784https://doi.org/10.1016/j.ijheatmasstransfer.2019.118784.